SCIENCE CHINA
Earth Sciences

•RESEARCH PAPER•

April 2020 Vol.63 No.4: 602–614
https://doi.org/10.1007/s11430-019-9481-9

Atmospheric deposition of ^{7}Be, ^{210}Pb and ^{210}Po during typhoons and thunderstorm in Shanghai, China and global data synthesis

Juan DU[1], Mark BASKARAN[2] & Jinzhou DU[1*]

[1] *State Key Laboratory of Estuarine and Coastal Research, East China Normal University, Shanghai 200241, China;*
[2] *Department of Geology, Wayne State University, Detroit 48202, USA*

Received April 23, 2019; revised September 5, 2019; accepted September 12, 2019; published online November 21, 2019

Abstract Atmospherically-delivered ^{7}Be, ^{210}Po and ^{210}Pb in bulk precipitation and air samples collected around the globe have provided valuable quantification on the rates of removal, as well as proportional mixing of attendant air masses; however, such studies during thunderstorm and typhoon events are limited. We report the first continuous time-series rainwater sampling and analysis of ^{7}Be, ^{210}Pb and ^{210}Po from two typhoons and one thunderstorm during 2015 summer in Shanghai. The depositional fluxes within individual rain events of typhoons and thunderstorms varied by a factor of 10 for ^{7}Be, 5.7 for ^{210}Pb, 7.4 for ^{210}Po, and 7.0 for ^{7}Be/^{210}Pb activity ratios (AR). Such large observed variations in the depositional fluxes of ^{7}Be, ^{210}Pb, ^{210}Po and ^{7}Be/^{210}Pb activity ratios were attributed to air masses injected from surrounding high pressure system adjoining the typhoon to low pressure system within the typhoon. Based on ^{7}Be/^{210}Pb activity ratios, we estimated the variations in the fraction of maritime and continental air masses into the typhoon. Observed constancy in the ^{210}Po/^{210}Pb AR indicates that the residence times of air masses contributing to the typhoon during heavy rain are similar. From a synthesis of global fallout of ^{7}Be and ^{210}Pb during pulse events (precipitation≥50 mm from single rainout event), we quantify the importance of pulse events in the atmospheric fallout of these radionuclides.

Keywords ^{7}Be, ^{210}Pb, ^{210}Po, Typhoon, Thunderstorm, Air masses intrusions

Citation: Du J, Baskaran M, Du J. 2020. Atmospheric deposition of ^{7}Be, ^{210}Pb and ^{210}Po during typhoons and thunderstorm in Shanghai, China and global data synthesis. Science China Earth Sciences, 63: 602–614, https://doi.org/10.1007/s11430-019-9481-9

1. Introduction

Atmospherically delivered beryllium-7 (^{7}Be, half-life, $T_{1/2}$ =53.3 d), lead-210 (^{210}Pb, $T_{1/2}$=22.3 yr) and polonium-210 (^{210}Po, $T_{1/2}$=138.4 d), have been widely used as tracers for studying atmospheric and surface earth processes such as time scales of atmospheric mixing (both horizontal and vertical), stability, and removal/transport of air masses, source tracking, rates of soil erosion and sediment accumulation/mixing in aqueous systems (e.g. Baskaran, 1995; Chen et al., 2016; Dibb, 2007; Du et al., 2008, 2015; Feely and Seitz, 1970; McNeary and Baskaran, 2007; Moore et al., 1973; Pham et al., 2011; Poet et al., 1972; Turekian and Graustein, 2003). Beryllium-7, a cosmogenic radionuclide, is produced primarily in the stratosphere and upper troposphere through cosmic-ray spallation with oxygen and nitrogen atoms and its flux to the earth's surface has a latitudinal dependence (Lal et al., 1958; Lal and Peters, 1967), hence its concentration in the atmosphere is expected to be higher at high altitudes above cloud condensation height. Due to its particle-reactivity, ^{7}Be is readily absorbed by aerosol particles in the air and eventually reach the earth's surface via wet and dry deposition. Though the ^{7}Be production rate at any given latitude in the atmosphere does not change with season, the intrusion of lower stratospheric air to the troposphere in mid-latitudes leads to enrichment of ^{7}Be

* Corresponding author (email: jzdu@sklec.ecnu.edu.cn)

depositional fluxes during late winter and early spring (Du et al., 2015; Feely et al., 1989; Yamamoto et al., 2006). In contrast to ^{7}Be, ^{210}Pb is a progeny of ^{222}Rn ($T_{1/2}$=3.82 d), which emanates primarily from the rocks and minerals on the earth's upper crust and embarks on its journey in the atmosphere via advection and diffusion. During its transit, it undergoes radioactive decay to ^{210}Pb which in turn decay to ^{210}Po via ^{210}Bi ($T_{1/2}$=5.0 d). The global radon emission fluxes from continents are ~76 to 106 times higher (1300–1800 Bq m^{-2} d^{-1}) compared to that from the oceanic surface (17 Bq m^{-2} d^{-1}) and hence ^{210}Pb flux strongly depends on longitude, whether it is above ocean or continent (Baskaran, 2011). Similar to ^{7}Be, both ^{210}Po and ^{210}Pb are also particle-reactive and are primarily removed by wet precipitation from the atmosphere (Baskaran, 2011; Du et al., 2008; Hirose et al., 2010; Pham et al., 2013).

The study area, Shanghai, is partially impacted by the Asian Monsoon system, with the northwest wind from the mainland of China with ^{222}Rn-enriched continental air masses and the southeast wind from the East China Sea (ECS) and the Pacific Ocean bringing ^{222}Rn-depleted maritime air masses (Bi, 2012; Du et al., 2015). As a result, the difference in the sources of these air masses is anticipated to reflect in the depositional fluxes of ^{210}Pb and possibly on ^{210}Po, but it is anticipated not to change so much for ^{7}Be. Moreover, from the analysis of the global ^{210}Pb fallout data set obtained from sampling locations with differing meteorological and geographical conditions, it was found that the ^{210}Pb depositional fluxes increase with distance from the coast in inland regions (distance from the coast >50 km) while in onshore regions (distance from the coast ≤50 km), the ^{210}Pb depositional fluxes varied considerably and increased with the increase in the amount of precipitation (Du et al., 2015).

All the earlier radionuclides studies were mostly focused on the bulk depositional fluxes over a longer periods of time (≥1 year) and concentrations in aerosols of ^{7}Be, ^{210}Pb and ^{210}Po (Dueñas et al., 2001; Kim et al., 2000; Lozano et al., 2011; Olsen et al., 1985; Persson and Holm, 2014; Pham et al., 2013; Su et al., 2003); however, studies focused on single rainout event are limited (Chen et al., 2016; McNeary and Baskaran, 2003, 2007; Tateda and Iwao, 2008; Uğur et al., 2011). Furthermore, to our knowledge, until now there is no published data on the temporal variations of the ^{7}Be/^{210}Pb and ^{210}Po/^{210}Pb activity ratios (AR) in rainout event from a single cloud cover corresponding to typhoon (also known as hurricane or cyclone) event. In this study, we report for the first time the temporal variations of the depositional fluxes of ^{7}Be, ^{210}Pb, ^{210}Po and how the AR of ^{7}Be/^{210}Pb and ^{210}Po/^{210}Pb evolve with time in precipitation from two typhoons and one heavy thunderstorm during summer 2015 in Shanghai, China. In conjunction with the air mass trajectory analysis, we evaluated the factors and processes that affect the radionuclides activities, depositional fluxes and their ARs of ^{7}Be, ^{210}Pb and ^{210}Po. The results from the present study will help us improving our understanding of the dynamics, sources of air mass injection into the hurricane-condensing cloud and whether ^{210}Po/^{210}Pb and ^{7}Be/^{210}Pb ARs can be utilized as a tracer for "older" air mass mixing with a relatively "younger" air mass.

2. Materials and methods

The sampling site was located on the roof of the State Key Laboratory of Estuarine and Coastal Research (SKLEC) building at the East China Normal University (ECNU), Shanghai, about 50 m above sea level (31°13′39″N, 121°23′56″E) and about 50 km from the nearest ECS coast (Figure 1).

An acid-cleaned 120 L polyethylene drum (0.26 m^2 surface area) was deployed on the roof to collect the precipitation samples. Between successive sampling, the drum was cleaned repeatedly with 6 M HCl and the rinsing was combined with sample for further processing. In this study, continuous rainwater samples from each of the three major precipitation events (RE-I, heavy thunderstorm with a total rainfall of 126.6 mm, 26–28 June 2015; RE-II, typhoon Chan-hom, No. 1509, 134.0 mm, 10–12 July 2015; and RE-III, typhoon Dujuan, No. 1521, 55.0 mm, 28–30 September 2015) were collected (Table 1, Figure 1).

The chemical processing of rainwater samples was similar to those described in our previous work (Du et al., 2015; McNeary and Baskaran, 2007). Briefly, rainwater samples were collected by a polyethylene drum with a surface area of 0.26 m^2 on the roof of the SKLEC building. After the collection, the samples were transferred to the laboratory, added ~1 dpm of ^{209}Po spike and subsequently reduced the volume to ~100 mL by evaporation at 90°C on a hot place. The solution of ~100 mL was subsequently filtered using a glass fiber filter with pore size of 0.45 μm and then evaporated again to ~60 mL. Concentrated NH_4OH was added to the solution to adjust the pH to about 1.5, and 0.3 g ascorbic acid, 1 mL 20% hydroxylamine hydrochloride and 1 mL 25% sodium citrate were added. Then polonium was electroplated on a nickel disc at 80–90°C with a magnetic stirrer on for 4 h. After the plating was complete, the nickel disc was rinsed with deionized water and ethanol, and then dried at room temperature. The activity of ^{210}Po was assayed using an alpha spectrometer (7200-08, Canberra Company). The plated solution was then evaporated to <5 mL and then transferred quantitatively to a counting vial for gamma counting using a HPGe gamma-ray detector system (ORTEC, GWL-120210-S) for ^{210}Pb (46.5 KeV, 4.25%) and ^{7}Be (477.6 KeV, 10.5%) assay. The calculation of the activities of ^{7}Be and ^{210}Pb assumes that there is no loss of these nuclides from evaporation till transfer to gamma counting vials.

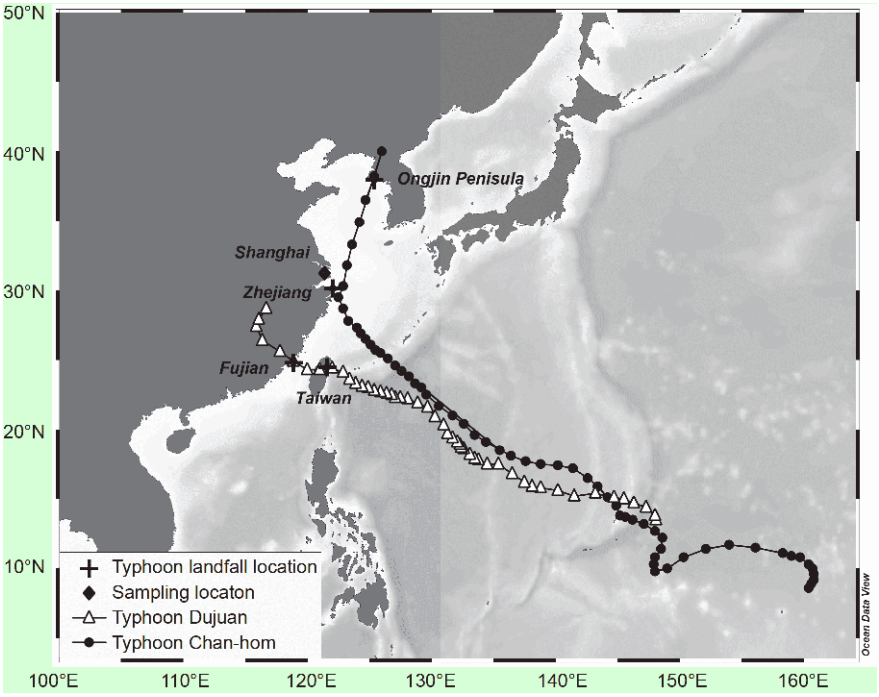

Figure 1 Sampling location and the tracks of typhoon Chan-hom and Dujuan.

Detailed calculations of the activities of ^{7}Be and ^{210}Pb are given in Du et al. (2015).

Air masses backward trajectory analyses were conducted with the Hybrid Single Particle Lagrangian Integrated Trajectory (HYSPLIT) model developed by the National Oceanic and Atmospheric Administration (NOAA). The backward trajectories were calculated at every sampling time interval (converted to the UTC time when using the HYSPLIT), including 72 h prior to the onset of heavy precipitation, at heights 1.5, 5 and 12 km above mean-sea-level. The initial altitude was set as 1.5 km for the back trajectories because this height is assumed to represent the base of precipitation cloud (Li, 2009) and the transportation of air masses is through lower atmospheric layer. The 12 km height was set as the top of the air mass trajectory height and the air mass transportation was assumed to be between the troposphere and the lower stratosphere (Peng et al., 2011) and the 5 km height was chosen to represent the air masses transportation in the middle troposphere.

3. Results

3.1 Meteorological conditions in Shanghai during summer

Annual precipitation in Shanghai is usually more than 1100 mm of which ~50% takes place during the raining season (June–August) when summer monsoon carries ^{222}Rn-depleted maritime air masses from the ECS. Samples from RE-I and RE-II were collected during the plum rain season (from 15th June to 13th July in 2015), when the Changjiang-Huaihe quasi-stationary front remained stable around the Changjiang Delta region, with the northern area of this stationary front having more continuous rain while in the southern area, the weather was found to be hot with high humidity, and with occurrence of many thunder storms. This is known as "the plum rain" season (or called "Meiyu" season in China and Baiu in Japan, Du et al., 2015; Meng et al., 2007; Yang et al., 2005). Precipitation during 2015 "plum rain" season (398 mm) was much higher than the average amount of 245 mm in the past ten years, and this plum rain season contributed about 45% of total precipitation during the flood season (877 mm, June-August, Shanghai water authority, 2015). There were totally 96 typhoons affected Shanghai from 1949 to 2015 and the numbers of typhoons in a year impacting Shanghai in the past varied (0 to 5 from 1949 to 2015, average=1.4±1.1, n=67). Only two typhoons occurred during 2015 (No. 1509 typhoon Chan-hom and No. 1521 typhoon Dujuan), with the tracks of these two typhoons and their landfall locations are shown in Figure 1.

Typhoon Chan-hom, the 9th named storm of the 2015 Pacific typhoon season, was a large and long-lived tropical cyclone that affected most countries in the western Pacific basin. Chan-hom developed from a tropical storm in the northwest Pacific Ocean on 30th June, and its wind speed increased while moving to the northwest and eventually became a typhoon on 3rd July. On 11th July, Chan-hom became very intense and made landfall in Zhejiang province

Table 1 Deposition fluxes and activities of ^{7}Be, ^{210}Pb and ^{210}Po measured in three rainout events in Shanghai, China in 2015[a)]

Sample ID	Sample collection nterval	Central pressure (hPa)	Time in hour (Precipitaion)	^{7}Be flux (Bq m^{-2} d^{-1})	^{7}Be (Bq L^{-1})	^{210}Pb flux (Bq m^{-2} d^{-1})	^{210}Pb (Bq L^{-1})	^{210}Po flux (mBq m^{-2} d^{-1})	^{210}Po (mBq L^{-1})	^{7}Be/^{210}Pb AR	^{210}Po/^{210}Pb AR
RE-I	20:00, 25 Jun–18:30, 26 Jun, 2015	–	22.5 (39.2)	26.8±2.2	0.64±0.05	4.32±0.56	0.10±0.01	348±8	8.50±0.17	6.21±0.55	0.082±0.012
	18:30, 26 Jun–19:20, 27 Jun 2015	–	22.5–48.3 (9.0)	11.5±1.0	1.37±0.11	3.04±0.42	0.15±0.01	282±8	13.3±0.8	3.77±0.71	0.095±0.007
	19:20, 27 Jun–16:20, 28 Jun 2015	–	48.3–69.3 (78.4)	19.5±1.3	0.22±0.02	5.23±0.75	0.06±0.01	432±20	4.83±0.17	3.74±0.32	0.083±0.015
RE-II	15:05, 10 Jul–9:00, 11 Jul, 2015	925	17.9 (27.4)	325±27	8.84±0.74	19.1±2.2	0.52±0.06	1650±17	50.7±0.5	17.0±1.5	0.096±0.012
	9:00–11:10, 11 Jul 2015	935	17.9–20.1 (11.8)	154±13	1.18±0.10	15.0±1.8	0.12±0.01	1405±50	10.8± 0.3	10.3±0.9	0.094±0.014
	11:10–13:00, 11 Jul 2015	945	20.1–21.9 (9.4)	32.9±2.7	0.27±0.02	13.5±1.8	0.11±0.01	1200±48	9.67±0.33	2.43±0.20	0.088±0.007
	13:00–16:00, 11 Jul 2015	945	21.9–24.9 (15.7)	36.4±3.4	0.29±0.03	6.69±0.94	0.05±0.01	628±27	5.00± 0.17	5.44±0.46	0.094±0.015
	16:00–18:00, 11 Jul 2015	955	24.9–26.9 (14.9)	31.4±2.9	0.18±0.02	4.17±0.66	0.02±0.01	223±12	1.83±0.17	7.54±0.63	0.079±0.013
	18:00–22:00, 11 Jul 2015	955	26.9–30.9 (17.6)	39.0±3.4	0.37±0.03	3.35±0.51	0.03±0.01	303±13	2.83± 0.17	11.6±1.0	0.089±0.010
	22:00, 11 Jul–7:30, 12 Jul 2015	960	30.9–40.4 (37.2)	89.2±7.4	0.95±0.08	5.64±0.97	0.06±0.01	620±8	5.83±0.17	15.8±1.3	0.097±0.005
RE-III	16:15, 28 Sep–10:40, 29 Sep 2015	935	18.4 (11.8)	15.3±1.4	1.00±0.09	3.83±0.49	0.25±0.03	267±20	17.3±1.3	4.00±0.43	0.069±0.009
	10:40–21:55, 29 Sep 2015	990	18.4–29.5 (11.8)	41.5±3.2	1.73±0.15	2.84±0.32	0.12±0.01	255±17	10.2±0.7	14.6±1.4	0.086±0.012
	21:55, 29 Sep–8:40, 30 Sep 2015	1005	29.5–40.4 (31.4)	31.8±2.7	0.45±0.04	9.22±1.23	0.13±0.02	840±67	11.8±1.0	3.45±0.29	0.090±0.011

a) Collection time interval is in China Standard Time (CST); central pressure at the beginning of each sample collection in two typhoons; data were obtained from the Department of water resources of Zhejiang Province, http://typhoon.zjwater.gov.cn/default.aspx; time elapsed from the beginning of precipitation and numbers in parenthesis denote amount of precipitation in millimeter.

(about 150 km away from Shanghai) and subsequently it moved to the northeast. On 13th July, Chan-hom made the landfall again at Ongjin peninsula, South Korea and then weakened into an extratropical cyclone. The storm dropped heavy rainfall, reaching 69.0 mm in Shanghai on 11th July after its first landfall (Shanghai water authority, 2015).

Typhoon Dujuan, the 21st named storm of the 2015 Pacific typhoon season, was the second most intense typhoon of the northwest Pacific Ocean in 2015. It started as a tropical storm and intensified into a typhoon on 25th September while moving to the northwest and eventually made landfall in Taiwan province (~720 km from Shanghai) on 28th September. Then it made the second landfall on Fujian province (~680 km from Shanghai) on 29th September. Though the two landfall places are farther away from Shanghai, Typhoon Dujuan still brought about 95.0 mm rainfall to Shanghai during 28th to 30th September (Shanghai water authority, 2015, http://www.shanghaiwater.gov.cn).

3.2 Temporal variations of amount of precipitation, activities of ^{7}Be, ^{210}Pb and ^{210}Po, their activity ratio(s) and depositional fluxes in three rainout events

In total three samples each in events RE-I and RE-III and seven samples in event RE-II were collected (Figure 2 and Table 1). Rainout event of RE-I lasted for about 3 days while both RE-II and RE-III lasted for about 2 days (Table 1). The amount of precipitation in each of the sample within a rainout event varied by a factor of about 9, 4 and 3 in RE-I, RE-II and RE-III, respectively (Table 1).

During RE-I, the depositional fluxes ranged from 11.5 to 26.8 Bq m^{-2} d^{-1} for ^{7}Be, 3.04 to 5.23 Bq m^{-2} d^{-1} for ^{210}Pb, and 282 to 432 mBq m^{-2} d^{-1} for ^{210}Po, respectively. The precipitation amount in RE-I decreased from 39.2 to 9.0 mm in the second sample and increased to 78.4 mm in the third sample and the corresponding depositional fluxes of all three radionuclides followed the same trend as the amount of precipitation, with the lowest value found in the second sample (Table 1). However, the specific activities (total activity deposited during the whole rain (Bq)/total volume (L) of water) of these three radionuclides showed a reverse trend with the highest value in the second sample, 1.37±0.11 Bq L^{-1} for ^{7}Be, 0.15±0.01 Bq L^{-1} for ^{210}Pb and 13.3±0.8 mBq L^{-1} for ^{210}Po. The total sampling time for Typhoon Chan-hom (RE-II) was about 40 h, with the total precipitation amount of 134 mm and the rainfall densities in seven samples ranged from 1.53 to 7.45 mm h^{-1} which were higher than those in RE-I and RE-III. In RE-II, the depositional fluxes of ^{7}Be, ^{210}Pb and ^{210}Po during the whole rainout event ranged from 30.5 to 325 Bq m^{-2} d^{-1}, 3.4 to 19.1 Bq m^{-2} d^{-1}, and 223 to 1650 mBq m^{-2} d^{-1}, respectively. The maximum depositional fluxes for all three radionuclides

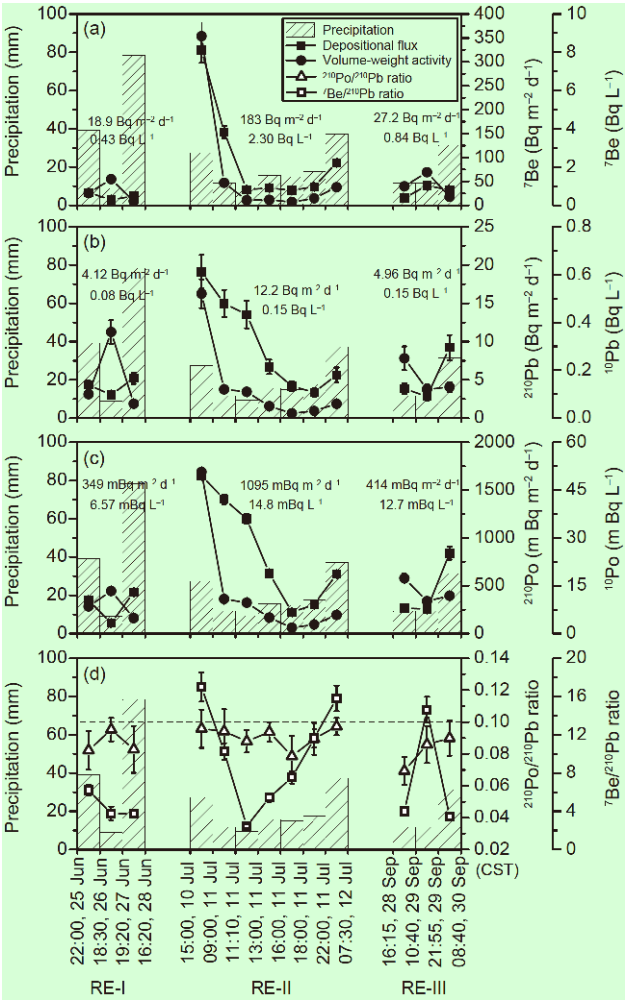

Figure 2 Depositional fluxes and activities of ^{7}Be (a), ^{210}Pb (b) and ^{210}Po (c) during three rainout events in summer 2015 (RE-I, RE-II and RE-III) in Shanghai, China. (d) ^{210}Po/^{210}Pb ratios and ^{7}Be/^{210}Pb ratios during three rainout events. The dash line in (d) represents for ^{210}Po/^{210}Pb is 0.10. The numbers represent the bulk depositional fluxes and the specific activities of the three radionuclides in three rainout events.

were observed in the first sample, and then they continued to decrease till end of the rainfall. The specific activities of ^{7}Be, ^{210}Pb and ^{210}Po in RE-II ranged from 0.18 to 8.84 Bq L^{-1}, 0.02 to 0.52 Bq L^{-1}, and 1.83 to 50.7 mBq L^{-1}, respectively with the highest value for all three radionuclides found in the first sample. The ^{7}Be activities in RE-II greatly decreased from 8.84 to 1.18 Bq L^{-1} in 2.2 hours and then it remained relatively constant between 0.18 and 0.37 Bq L^{-1} (mean: 0.28±0.07 Bq L^{-1}, n=4) from 21.9 to 30.9 hours after the beginning of rainfall, while both ^{210}Po and ^{210}Pb activities continuously decreased from beginning till 26.9 hours. Note that the specific activities of all three radionuclides increased in RE-II in the last two samples. In RE-III, the increase in the amount of precipitation in the third sample resulted in the highest depositional fluxes of 9.22±1.23 Bq m^{-2} d^{-1} for ^{210}Pb and 840±67 mBq m^{-2} d^{-1} for ^{210}Po, while the lowest value was found in the second sample with 2.84±0.32 Bq m^{-2} d^{-1} for ^{210}Pb and 255±17 mBq m^{-2} d^{-1} for ^{210}Po. The specific activities of ^{7}Be exhibited similar trend as the depositional fluxes, with the highest value of 1.73±0.15 Bq L^{-1} in the second sample followed by a sharp decline to 0.45±0.04 Bq L^{-1} in the third sample due to a large increase in the amount of precipitation (dilution effect). However, the highest specific activities of ^{210}Pb and ^{210}Po were observed in the first sample, 0.25±0.03 Bq L^{-1} and 17.3±1.3 mBq L^{-1}, respectively, followed by subsequent decrease to the lowest value of 0.12±0.01 Bq L^{-1} (^{210}Pb) and 10.2±0.7 mBq L^{-1} (^{210}Po) in the second sample, then with a marginal increase in the third sample even though the precipitation amount was much higher.

3.3 The bulk depositional fluxes of ^{7}Be, ^{210}Pb and ^{210}Po in three rainout events

The bulk depositional fluxes of the three radionuclides in RE-I, RE-II and RE-III were 18.9, 183 and 27.2 Bq m^{-2} d^{-1} for ^{7}Be, 4.12, 12.2 and 4.96 Bq m^{-2} d^{-1} for ^{210}Pb, and 349, 1095 and 414 mBq m^{-2} d^{-1} for ^{210}Po, respectively. In all three rainout events, the logarithmic correlation was observed between cumulative depositional fluxes of radionuclides and the elapsed time (Figure 3a, 3d and 3e). The specific activities for these three radionuclides in RE-I, RE-II and RE-III were 0.43, 2.30 and 0.84 Bq L^{-1} for ^{7}Be, 0.08, 0.15 and 0.15 Bq L^{-1} for ^{210}Pb and 6.57, 14.8 and 12.7 mBq L^{-1} for ^{210}Po, respectively (Figure 3b, 3e and 3h). In RE-II, well-defined negative exponential relationship between cumulative ^{7}Be, ^{210}Pb and ^{210}Po activities and elapsed time can be observed (Figure 3e), in RE-III, such relationship can be observed for ^{210}Pb and ^{210}Po (Figure 3h), while in RE-I, no such relationship was found in any of three radionuclides. Among these three rainout events, RE-II which was caused by the Typhoon Chan-hom, had the maximum rainfall intensity as well as the highest depositional fluxes and specific activities for all three radionuclides in spite of their different origins and transport pathways in the atmosphere. In particular, for ^{7}Be, the specific activity in RE-II was about 5 times higher in RE-I and 3 times higher in RE-III.

4. Discussions

4.1 Sources and transport of air masses during typhoons and thunderstorm using radionuclides

It is well known that radon is not scavenged from the atmosphere by precipitation events, but only its progeny (^{210}Pb and ^{210}Po) are removed from the atmospheric air. Generally, the radionuclides are primarily removed from the atmosphere through both by washout (in-cloud scavenging) and rainout (scavenging below cloud cover) processes. The activities ^{7}Be, ^{210}Pb and ^{210}Po in rainwater are generally higher

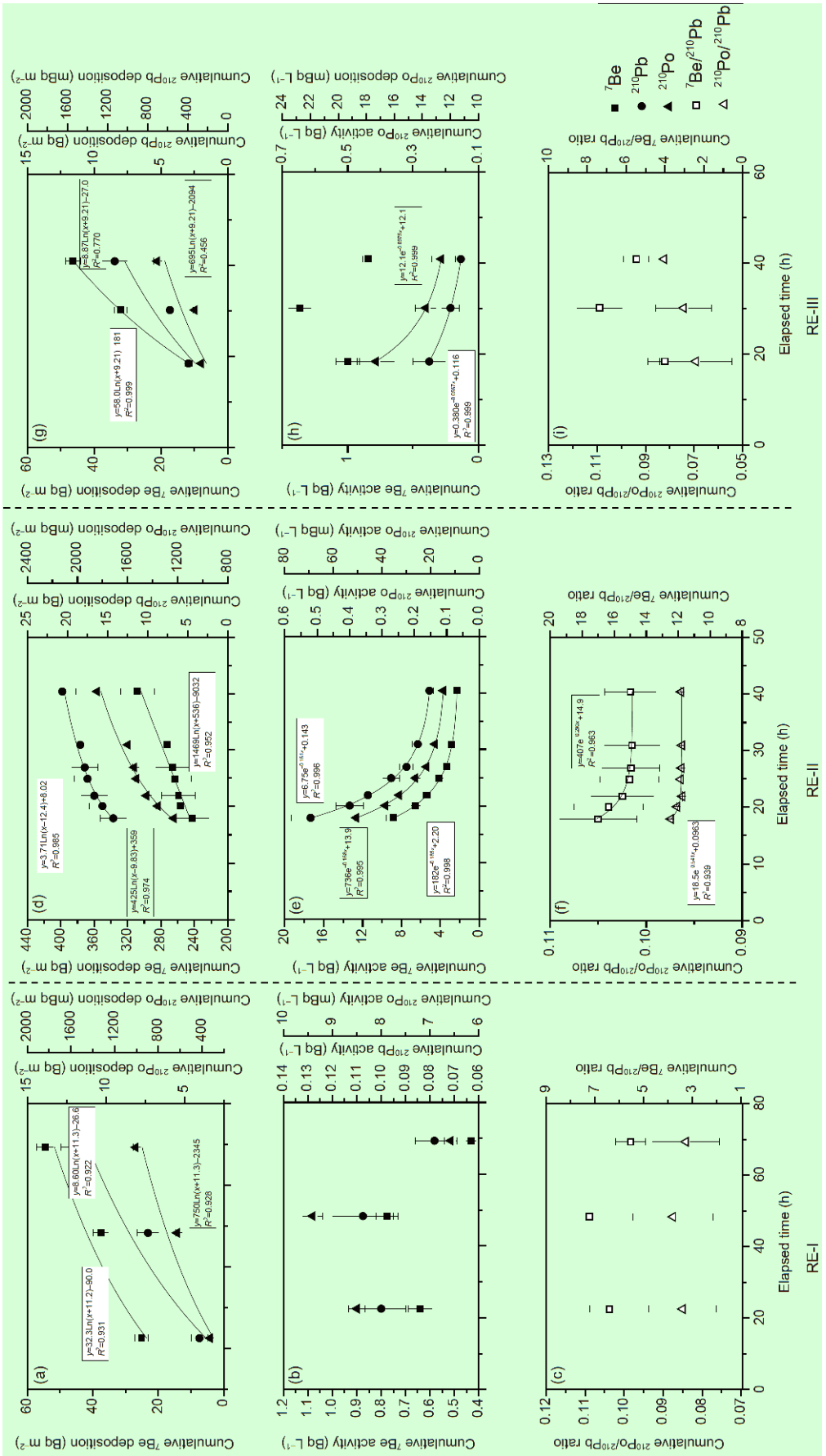

Figure 3 Cumulative depositional fluxes, activities and activity ratios versus elapsed time in RE-I ((a)–(c)), RE-II ((d)–(f)), and RE-III ((g)–(i)) in shanghai, China.

in the early stages of rainfall, for example, in RE-II, the fisrt sample contributed only 20% of the total amount of precipitation but constituted much larger fraction of total depositional fluxes (79% for ^{7}Be, 69% for ^{210}Pb and 67% for ^{210}Po) and subsequently decreased due to dilution effect. If a certain air mass is undergoing condensation without any additional input from the surrounding air masses via lateral injection and/or folding from upper troposphere-lower stratosphere, the specific activities of all three radionuclides in one rainout event are anticipated to decrease systematically from the beginning. However, if one or more air masses with distinctive characteristics such as maritime, continental and/or upper atmospheric air masses intrude, the ARs of ^{7}Be/^{210}Pb and ^{210}Po/^{210}Pb in the condensing cloud are expected to vary (Figure 4). For example, compared with maritime air mass which has lower ^{210}Pb activity, continental air mass derived from the same or similar latitude is expected to have lower ^{7}Be/^{210}Pb AR (due to higher ^{210}Pb activity per m^{3} air but similar ^{7}Be activity). If there is subduction of air mass from altitude above the cloud condensation height (the middle-upper troposphere and lower stratosphere), then the residence time of the subducting air mass from aloft is expected to be longer, with higher ^{7}Be specific activity (and hence higher ^{7}Be/^{210}Pb AR). In the case of ^{210}Po/^{210}Pb AR, the aerosols above cloud condensation height are expected to have higher ^{210}Po/^{210}Pb AR, due to older air mass, so that the vertical air mass sinking into low-pressure system (such as the eye of a typhoon) is expected to result in higher ^{210}Po/^{210}Pb AR.

In RE-I, ^{7}Be/^{210}Pb ARs decreased from 6.21 in the first sample to 3.77 in the second sample and remained constant thereafter. Such a high ratio in the first precipitation sample in RE-I was due to the higher ^{7}Be depositional flux than ^{210}Pb. Prior to the onset of heavy precipitation event, it appears that upper air mass downdraft resulted in higher ^{7}Be (relative to ^{210}Pb) in aerosols below cloud condensation height. Once those excess ^{7}Be are removed by first precipitation, then, the ^{7}Be/^{210}Pb ratio had remained constant (Table 1). Based on the air-mass backward trajectory analysis (Figure 5a), there was no significant change in the

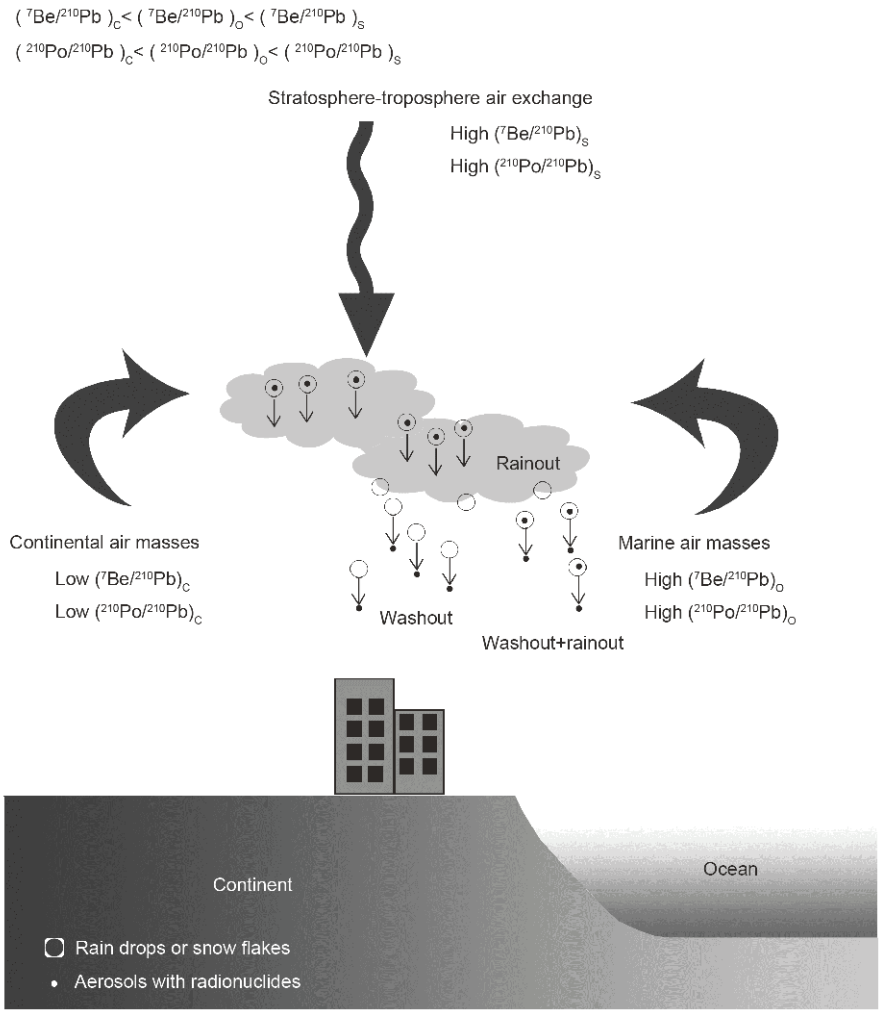

Figure 4 The schematic diagram of air masses intrusions into the condensing cloud at the coastal area.

sources of air masses during RE-1. The air masses at 12 km height appeared to have been derived from continents in the northwestern China while air masses in the middle and lower troposphere from southern China. However, the heavy wind is a result of higher pressure gradient (PG) between a high-pressure point and a low-pressure point. During periods of heavy wind, air mass flows from high pressure to low pressure (e.g. into cloud condensation height (CCH) from aloft), resulting in the vertical downward movement of air mass. In such a case, it would have resulted in higher ^{210}Po/^{210}Pb AR, as evidenced from observed increase in the ^{210}Po/^{210}Pb AR, from 0.082±0.012 to 0.095±0.007 in RE-I (Table 1, Figure 2).

During RE-II, typhoon Chan-hom developed into a super typhoon from heavy thunderstorm with a central pressure of 925 hectopascal (hPa) at 15:05 on 10th July, 2015. At this moment, the distance between Shanghai and the typhoon center was about 600 km (Department of Water Resources of Zhejiang Province, http://typhoon.zjwater.gov.cn/default.aspx), and the typhoon Chan-hom hadn't impacted Shanghai greatly. HYSPLIT simulations indicated that the source of air masses at 12 km height were still from the inland areas while air masses at lower-middle troposphere were from the ECS (Figure 5b). Thereafter, the distance between Shanghai and the typhoon center continuously decreased, which impacted precipitation in Shanghai. Typhoon Chan-hom brought ^{210}Pb-depleted air masses from the Pacific Ocean (PO) to Shanghai, as can be seen from the northward spiraling air masses at 12 km from the Pacific, which was similar to the air masses in the middle and lower troposphere (Figure 5b). Moreover, the pressure gradually increased from 935 to 960 hPa from the 3rd to 6th sample (in 9 hours), but the ^{7}Be depositional fluxes remained relatively constant (35.2±3.8 Bq m^{-2} d^{-1}); meanwhile, the ^{210}Pb depositional fluxes decreased from 13.5 to 3.35 Bq m^{-2} d^{-1}. The depositional fluxes of ^{7}Be and ^{210}Pb as well as the ^{7}Be/^{210}Pb AR indicate injection of extraneous air masses into typhoon, due to pressure gradient between the eye of the typhoon and the adjoining air mass outside the periphery of the typhoon. Furthermore, the temporal variations of ^{7}Be/^{210}Pb AR during the precipitation could also indicate intrusion of variable fractions of continental and maritime air masses to Shanghai. Such inflows of air masses with different characteristics resulted in the increase of ^{7}Be depositional fluxes and ^{210}Pb by the end of the rainfall (Figure 2).

During RE-III (Typhoon Dujuan), the observed ^{7}Be/^{210}Pb AR variation clearly indicated changes in air mass sources during the precipitation process. The steep increase in ^{7}Be flux along with a slight decrease in ^{210}Pb flux from the first sample to the second sample indicate that the relative fraction of maritime and continental air masses drawn into the typhoon's low pressure system had changed. Prior to the beginning of the precipitation, air masses in both upper and middle troposphere were continental air masses derived from inland China, while those at the 1.5 km height were maritime air masses from the Pacific Ocean (Figure 5c). Soon after the beginning of first sampling, typhoon Dujuan made the landfall in Taiwan province and moved southward to make the second landfall at Fujian province, subsequently, the sources and transport pathways of air masses at middle troposphere changed from inland China to maritime air masses from the ECS during these two landfalls (Figure 5c) After the second landfall at Fujian province, air masses transport pathways at 12 km height were affected by the typhoon and changed into the maritime air masses coming from south of Shanghai, resulting in the decrease of ^{210}Pb depositional flux and ^{210}Pb activity in the second sample. Correspondingly, the air pressure changed from 935 hPa in the first sample to 990 hPa in the second sample (within 11.8 hours), again indicating input of maritime air masses with lower ^{210}Pb activity. From the second to the third sample, the ^{7}Be activity decreased by 79% but both the ^{210}Pb and ^{210}Po activities were almost constant, suggesting the continuous intrusion of air masses bringing ^{210}Pb and ^{210}Po below the condensation cloud. Due to sampling limitation such as limited sample volume and overlong sampling periods, we are unable to quantitatively estimate the fractional inputs of both continental and oceanic air masses in the present study, and future studies involving simultaneous measurements of ^{7}Be, ^{210}Po and ^{210}Pb in aerosols and precipitation are required to quantify the fractional amounts these two sources of air masses. The increase of ^{210}Pb depositional flux at the end of RE-III was attributed to higher fraction of continental air mass, and the relatively higher ^{210}Po/^{210}Pb AR in this sample could be attributed to the presence of very fine terrigenous dust in which both ^{210}Pb and ^{210}Po are expected to be in secular equilibrium. However, this difference may not be significant, as within 2 standard deviations of the propagated error on the ^{210}Po/^{210}Pb ARs all samples are about the same.

During all three rainout events, the variations in the ^{210}Po/^{210}Pb ARs were not significant, within a difference of 0.012 in RE-I, 0.017 in RE-II and 0.021 in RE-III, suggesting that the residence times of aerosols, both inside the cloud and added from the surrounding air into the tornado-cloud, were similar in age during the rainout event (ranged 20.6–27.8 d, with the average of 25.3 d).

4.2 Insights into the depositional fluxes of ^{7}Be and ^{210}Pb from pulse rainout events-synthesis of global data set

Pulse rainout events like RE-I, RE-II and RE-III in this study not only bring large amounts of rainfall but also contribute significantly to the deposition of radionuclides like ^{7}Be, ^{210}Pb and ^{210}Po. In 2015, RE-I, RE-II and RE-III together brought 18.6% of the total annual precipitation, but deposited about 28% and 11% of the total annual bulk de-

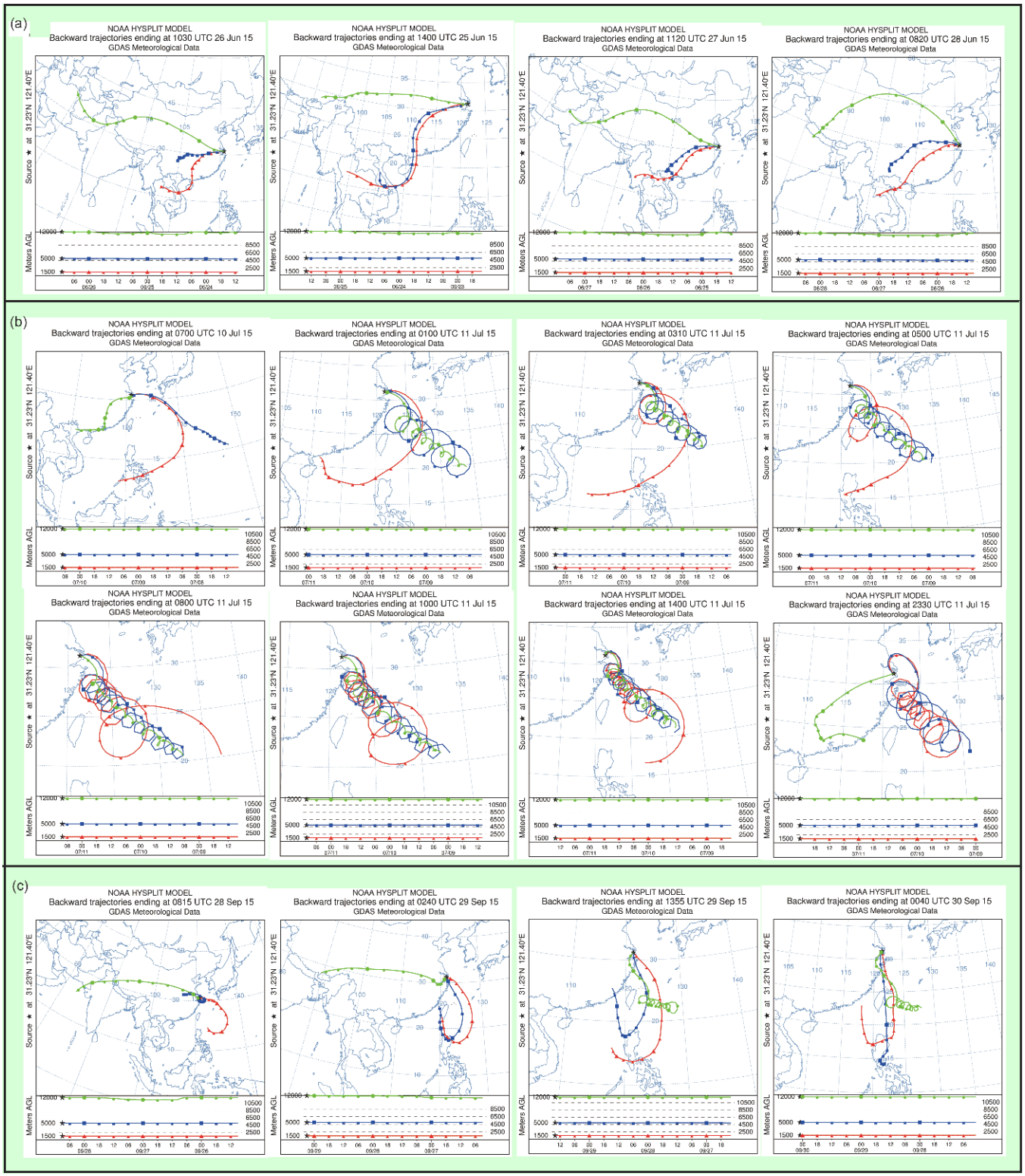

Figure 5 Air masses backward trajectory analyses of the three rainout events. (a) RE-I; (b) RE-II; and (c) RE-III.

positional fluxes of ^{7}Be and ^{210}Pb, respectively (Table 2). A summary of the percentages the total annual rainfall, bulk depositional fluxes of ^{7}Be and ^{210}Pb during pulse rainout events (≥50 mm precipitation from single rainout event) around the world are summarized in Table 2. It can be seen that these pulse rainout events significantly contributed to the annual depositional fluxes of both ^{7}Be and ^{210}Pb, especially the rainout events caused by typhoon. For example,

typhoon Melor brought 9.2% of annual ^{7}Be depositional flux to California, USA in 2010 (Conaway et al., 2013) compared to 17.9% of the total amount of precipitation; rainout events caused by typhoon brought 16% of total ^{7}Be depositional flux and 12% of total ^{210}Pb depositional flux compared to 31% of the total amount of precipitation to Nankang, Taiwan province during 9-year time series study (1996 to 2005, Huh et al., 2006); in our present study, RE-II caused by typhoon Chan-hom brought 21% of annual ^{7}Be depositional flux and 5.6% of annual ^{210}Pb depositional flux to Shanghai. Note that there is no data on the time-series measurements of these nuclides in typhoons in published literature. The relatively lower percentage contributions of radionuclide fluxes compared to the fractional amounts of total precipitation were possibly caused by the dilution effect. Furthermore, it is likely that a major fraction of the water vapor in typhoon is recycled prior to arrival at the coastal station resulting in ^{7}Be-depleted and ^{210}Pb-depleted low-latitude maritime air masses. A strong linear correlation between the percentages of annual ^{7}Be depositional flux and the percentages of annual ^{210}Pb depositional flux in the pulse rainout events is observed in Figure 6 (R^2=0.60, p<0.01); however a slope of 1.60±0.27 indicates that these pulse rainout events brought more ^{7}Be than ^{210}Pb, suggesting a relatively enhanced convective mixing or stratosphere-troposphere exchange during these rainout events (Wang, 2014).

To quantify the variations in the depositional fluxes of ^{7}Be and ^{210}Pb in pulse rainout events, the precipitation-normalized enrichment factors (α) were calculated in this study. The α value was calculated from the following equation, which is modified from Baskaran (1995):

$$\alpha = P_f / P_p, \quad (1)$$

where P_f and P_p are the percentages of annual depositional flux and amount of precipitation for single pulse rainout events, respectively. Values of α>1.0 indicate that the depositional fluxes were higher than expected from the amount of precipitation, and α<1.0 indicate depletion of the depositional fluxes of the nuclides. The precipitation-normalized enrichment factors (α) values of ^{7}Be and ^{210}Pb in pulse rainout events ranged from 0.06 to 6.10 and from 0.09 to 2.07, respectively (Table 2). As shown in Figure 7, the α values of both ^{7}Be and ^{210}Pb were lower than 1.0 in most pulse rainout events. In 27 out of 42 and 28 out of 36 pulse rainout events had α<1.0 for ^{7}Be and ^{210}Pb, respectively, indicating that in most pulse rainout events, the depositional fluxes of ^{7}Be and ^{210}Pb were lower relative to the amount of precipitation, such results were expected and were due to the dilution effect by the large amounts of precipitation (Huh et al., 2006). In our previous studies, it was reported that the α values of both ^{7}Be and ^{210}Pb in summer and fall (when precipitation amount was large) in Shanghai were lower than 1.0 during 6-year study (Du et al., 2015). However, the α>1.0

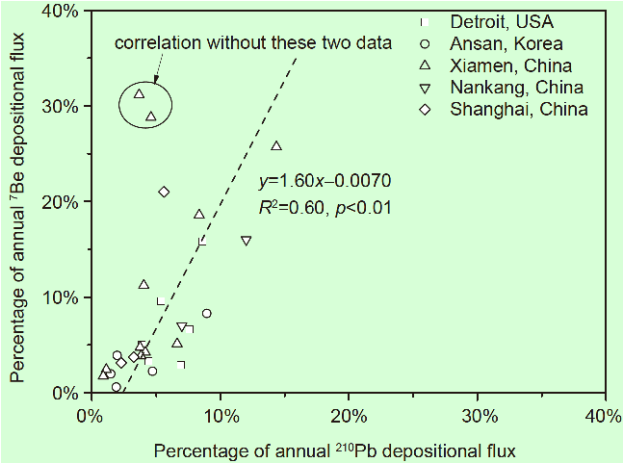

Figure 6 Percentages of annual ^{7}Be depositional flux plotted against percentages of annual ^{210}Pb depositional flux.

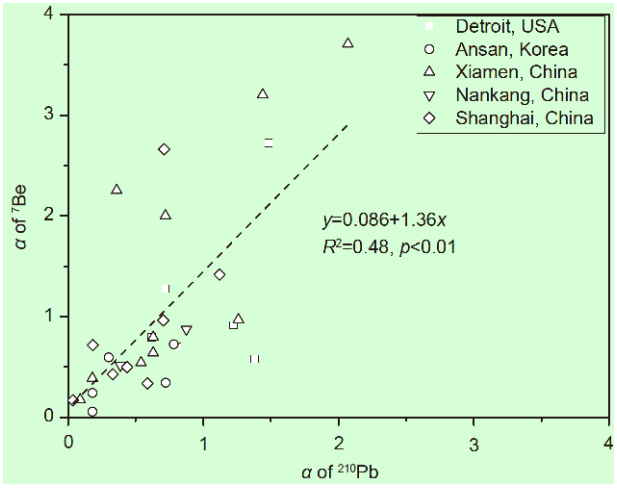

Figure 7 The precipitation-enrichment factors of ^{7}Be plotted against the precipitation-enrichment factors of ^{210}Pb for the pulse rainout events.

for both radionuclides could still been found in some stations (Figure 7), showing that there were enrichments of ^{7}Be or ^{210}Pb in some pulse rainout events, which might have been caused by the intrusions of air masses (vertical or horizontal transportation) during the rainfall; more studies during pulse precipitation in coastal and open ocean stations, as well as time-series measurements of δ^{18}O and δ^{2}H are needed to better understand the intrusions of these air masses (e.g. Gat and Matsui, 1991; Yamanaka et al., 2002; Tanoue et al., 2017). It can also be observed that the α values of ^{7}Be were higher than ^{210}Pb in 72% of all pulse rainout events (23 out of 32), and the slope of the correlation between α of ^{7}Be and ^{210}Pb is 1.36±0.27, indicating again that these pulse rainout events brought more ^{7}Be than ^{210}Pb as mentioned above. The α values of ^{210}Pb at the coastal stations like Ansan, Xiamen, Nankang, and Shanghai were lower than those at Detroit, which is an inland city, indicating the intrusion of ^{210}Pb-

Table 2 Percentages of bulk depositional fluxes and precipitation-normalized enrichment factors (α) of ^{7}Be and ^{210}Pb during pulse rainout events[a)]

Location	Sample	Percent of annual precipitation	^{7}Be		^{210}Pb		References
			Percent of annual flux	α	Percent of annual flux	α	
Detroit, USA	RWB 1	5.8%	15.8%	2.72	8.6%	1.48	McNeary and Baskaran, 2003
	RWB 10	7.5%	9.6%	1.28	5.4%	0.72	
	RWB 16	6.3%	5.0%	0.79	3.9%	0.62	
	RWB 20	3.6%	3.3%	0.92	4.4%	1.22	
	RWB 21	9.4%	6.6%	0.70	7.6%	0.81	
	RWB 25	5.0%	2.9%	0.58	6.9%	1.38	
Ansan, Korea	5 heavy rainfalls with more than 50 mm precipitation amount in 1992	6.5%	2.2%	0.34	4.7%	0.72	Kim et al., 1998
		6.6%	3.9%	0.60	2.0%	0.30	
		11.4%	8.3%	0.73	8.9%	0.78	
		10.5%	0.6%	0.06	1.9%	0.18	
		8.2%	2.0%	0.24	1.5%	0.18	
Xiamen, China*	11 heavy rainfalls more than 50 mm precipitation amount from 2004 to 2005	5.1%	31.2%	6.10	3.7%	0.72	Chen et al., 2016; Jia et al., 2003
		5.3%	5.1%	0.97	6.6%	1.26	
		5.6%	11.2%	2.00	4.0%	0.72	
		5.8%	18.6%	3.20	8.3%	1.44	
		6.0%	4.7%	0.80	3.8%	0.63	
		6.2%	2.4%	0.39	1.1%	0.18	
		6.6%	4.2%	0.64	4.2%	0.63	
		6.9%	25.7%	3.71	14.3%	2.07	
		7.1%	3.8%	0.54	3.8%	0.54	
		9.9%	1.7%	0.17	0.9%	0.09	
		12.8%	28.8%	2.25	4.6%	0.36	
California, USA	Typhoon Melor in 2010	17.9%	9.2%	0.51	–		Conaway et al., 2013
	6 extra-tropical storms in 2010	3.1%	5.2%	1.68	–		
		7.0%	6.3%	0.90	–		
		9.2%	9.9%	1.07	–		
		3.2%	3.8%	1.18	–		
		5.8%	3.7%	0.65	–		
		5.8%	4.2%	0.73	–		
Nankang, China*	Rainfalls caused by typhoon during 9 year time series from 1996 to 2005	31.0%	16.0%	0.52	12.0%	0.39	Huh et al., 2006
	Rainfalls in plum season during 9 year time series from 1996 to 2005	8.0%	7.0%	0.88	7.0%	0.88	
Ahemedabad, India	5 heavy rainfalls with more than 50 mm precipitation amount in 2000 and 2001	7.0%	–		6.5%	0.93	Rastogi and Sarin, 2008
		7.0%	–		1.7%	0.24	
		7.5%	–		2.7%	0.36	
		14.0%	–		20.5%	1.47	
		14.0%	–		7.0%	0.50	
San Luis, Argentina	3 heavy rainfalls with more than 50 mm precipitation amount in 2007 and 2008	7.7%	8.1%	1.05	–	–	Ayub et al., 2009
		7.9%	10.1%	1.28	–	–	
		8.1%	10.5%	1.30	–	–	
Shanghai, China	RE-I	7.5%	3.7%	0.50	3.3%	0.44	This study
	RE-II	7.9%	21.0%	2.66	5.6%	0.71	
	RE-III	3.2%	3.1%	0.96	2.3%	0.70	
	5 heavy rainfalls with more than 50 mm precipitaiton amount in 2010	4.9%	2.1%	0.43	1.6%	0.33	Kong, 2012
		5.0%	3.6%	0.72	0.9%	0.18	
		5.5%	0.9%	0.17	0.2%	0.04	
		6.2%	8.8%	1.42	6.9%	1.12	
		6.2%	2.1%	0.34	3.7%	0.59	

a) * pulse rainout events data in Xiamen, China were collected in 2004 and 2005 (Chen et al., 2016), but the annual depositional fluxes in 2002 were taken from Jia et al. (2003). Data in Nankang, Taiwan province were the summation of 9 year time series data.

depleted maritime air masses when condensation took place within the cloud cover at these coastal stations. The variations in the depositional fluxes of ^{7}Be, ^{210}Po, ^{210}Pb and activity ratios (^{210}Po/^{210}Pb and ^{7}Be/^{210}Pb) are anticipated to provide insight on the sources and pathways of air masses that feed into typhoons and heavy thunderstorms. Furthermore, this study paves the way for a better understanding of the deposition characteristics of other atmospherically delivered stable elements that behave similar to ^{7}Be and ^{210}Pb (McNeary and Baskaran, 2003).

5. Conclusions

From the first time-series measurements of depositional fluxes, specific activities of ^{7}Be, ^{210}Pb and ^{210}Po and their ARs (^{7}Be/^{210}Pb and ^{210}Po/^{210}Pb) from one thunderstorm and two typhoons in Shanghai, China, we draw the following conclusions: (1) three pulse rainout events contributed to about 28% and 11% of the total annual bulk depositional fluxes of ^{7}Be and ^{210}Pb, respectively to Shanghai; (2) there are large temporal variations of the depositional fluxes and specific activities of ^{7}Be, ^{210}Pb and ^{210}Po as well as the activity ratios of ^{7}Be/^{210}Pb within one rainout event; (3) generally, the depositional fluxes and specific activities of ^{7}Be, ^{210}Pb and ^{210}Po are higher at the beginning of the rainfall, although there are large variations in these values; (4) the variations of ^{7}Be/^{210}Pb ratios during rainout events indicate varying sources of air masses contributing to the rainout and events as well varying fraction of continental and maritime air mass intruding from the surrounding area into the low pressure system of the typhoon; (5) temporal variations in the ^{210}Po/^{210}Pb AR have relatively smaller range of variations (0.083±0.014), indicating that the "age" of air masses that undergo condensation for all three events are similar; and (6) from a synthesis of the global data of the depositional flux of ^{7}Be and ^{210}Pb in pulse rainout events, we observe that the dilution effect by the large amounts of precipitation would deplete the radionuclides, resulting in lower fraction of total annual depositional flux compared to the fraction of total annual precipitation.

Acknowledgements *The sample collection and analysis reported in this paper were conducted from the SKLEC/ECNU. Data synthesis and writing of this manuscript was conducted during research study of Juan Du at Wayne State University. This work was supported by the China National Key Research and Development Program (Grant No. 2016YFA0600904), the Outstanding Doctoral Dissertation Cultivation Plan of Action by the ECNU (Grant No. PY2015027) and the ECNU for Overseas Scholars and the China Scholarship Council (Grant No. 201606140124). Mark Baskaran acknowledges the travel support to SKLEC 111 Project (Grant No. B08022).*

References

Ayub J J, Di G D E, Velasco H, Huck H, Rizzotto M, Lohaiza F. 2009. Short-term seasonal variability in ^{7}Be wet deposition in a semiarid ecosystem of central Argentina. J Environ Radioact, 100: 977–981

Baskaran M. 1995. A search for the seasonal variability on the depositional fluxes of ^{7}Be and ^{210}Pb. J Geophys Res, 100: 2833–2840

Baskaran M. 2011. Po-210 and Pb-210 as atmospheric tracers and global atmospheric Pb-210 fallout: A review. J Environ Radioact, 102: 500–513

Bi Q. 2012. The disequilibrium of ^{234}Th/^{238}U and ^{210}Po/^{210}Pb in the Changjiang estuary and adjacent sea: A case study of tracing the export of particulate organic carbon (in Chinese with English abstract). Dissertation for Master's Degree. Shanghai: East China Normal University

Chen J, Luo S, Huang Y. 2016. Scavenging and fractionation of particle-reactive radioisotopes ^{7}Be, ^{210}Pb and ^{210}Po in the atmosphere. Geochim Cosmochim Acta, 188: 208–223

Conaway C H, Storlazzi C D, Draut A E, Swarzenski P W. 2013. Short-term variability of ^{7}Be atmospheric deposition and watershed response in a Pacific coastal stream, Monterey Bay, California, USA. J Environ Radioact, 120: 94–103

Dibb J E. 2007. Vertical mixing above Summit, Greenland: Insights into seasonal and high frequency variability from the radionuclide tracers ^{7}Be and ^{210}Pb. Atmos Environ, 41: 5020–5030

Du J, Zhang J, Zhang J, Wu Y. 2008. Deposition patterns of atmospheric ^{7}Be and ^{210}Pb in coast of East China Sea, Shanghai, China. Atmos Environ, 42: 5101–5109

Du J, Du J, Baskaran M, Bi Q, Huang D, Jiang Y. 2015. Temporal variations of atmospheric depositional fluxes of ^{7}Be and ^{210}Pb over 8 years (2006–2013) at Shanghai, China, and synthesis of global fallout data. J Geophys Res-Atmos, 120: 4323–4339

Dueñas C, Fernández M C, Carretero J, Liger E, Cañete S. 2001. Atmospheric deposition of ^{7}Be at a coastal Mediterranean station. J Geophys Res, 106: 34059–34065

Feely H W, Seitz H. 1970. Use of lead 210 as a tracer of transport processes in the stratosphere. J Geophys Res, 75: 2885–2894

Feely H W, Larsen R J, Sanderson C G. 1989. Factors that cause seasonal variations in Beryllium-7 concentrations in surface air. J Environ Radioact, 9: 223–249

Gat J R, Matsui E. 1991. Atmospheric water balance in the Amazon Basin: An isotopic evapotranspiration model. J Geophys Res, 96: 13179

Hirose K, Kikawada Y, Doi T, Su C C, Yamamoto M. 2010. ^{210}Pb deposition in the far East Asia: Controlling factors of its spatial and temporal variations. J Environ Radioact, 102: 514–519

Huh C A, Su C C, Shiau L J. 2006. Factors controlling temporal and spatial variations of atmospheric deposition of ^{7}Be and ^{210}Pb in northern Taiwan. J Geophys Res, 111: D16304

Jia C, Liu G, Yang W, Zhang L, Huang Y. 2003. Atmospheric depositional fluxes of ^{7}Be and ^{210}Pb at Xiamen (In Chinese with English abstract). J Xiamen Univ-Nat Sci, 42: 352–357

Kim G, Hussain N, Scudlark J R, Church T M. 2000. Factors Influencing the Atmospheric Depositional Fluxes of Stable Pb, ^{210}Pb, and ^{7}Be into Chesapeake Bay. J Atmos Chem, 36: 65–79

Kim S, Hong G, Baskaran M, Park K, Chung C, Kim K. 1998. Wet removal of atmospheric ^{7}Be and ^{210}Pb at the Korean Yellow Sea Coast. The Yellow Sea, 4: 58–68

Kong R. 2012. The characteristics and controlling factors of ^{7}Be and ^{210}Pb deposition in Shanghai (In Chinese with English abstract). Dissertation for Master's Degree. Shanghai: East China Normal University

Lal D, Peters B. 1967. Cosmic ray produced radioactivity on the earth. In: Sitte K, ed. Kosmische Strahlung II/Cosmic Rays II. New York: Springer Berlin Heidelberg. 551–612

Lal D, Malhotra P K, Peters B. 1958. On the production of radioisotopes in the atmosphere by cosmic radiation and their application to meteorology. J Atmos Terr Phys, 12: 306–328

Li Y. 2009. Acid deposition responsing of meteorological elements and air mass trajectories in Liaozhong station (in Chinese with English abstract). Dis-

sertation for Master's Degree. Shangdong: Shandong Normal University
Lozano R L, San Miguel E G, Bolívar J P, Baskaran M. 2011. Depositional fluxes and concentrations of ^{7}Be and ^{210}Pb in bulk precipitation and aerosols at the interface of Atlantic and Mediterranean coasts in Spain. J Geophys Res, 116: D18213
McNeary D, Baskaran M. 2003. Depositional characteristics of ^{7}Be and ^{210}Pb in southeastern Michigan. J Geophys Res, 108: 4210
McNeary D, Baskaran M. 2007. Residence times and temporal variations of ^{210}Po in aerosols and precipitation from southeastern Michigan, United States. J Geophys Res, 112: D04208
Meng F, Kang J, Wang T, An Y, Yuan W. 2007. Characteristics and influence factors of summer precipitation temporal and spatial distribution in Shanghai during one hundred years (in Chinese with English abstract). Meteorol Environ Sci, 30: 14–19
Moore H E, Poet S E, Martell E A. 1973. ^{222}Rn, ^{210}Pb, ^{210}Bi, and ^{210}Po profiles and aerosol residence times versus altitude. J Geophys Res, 78: 7065–7075
Olsen C R, Larsen I L, Lowry P D, Cutshall N H, Todd J F, Wong G T F, Casey W H. 1985. Atmospheric fluxes and marsh-soil inventories of ^{7}Be and ^{210}Pb. J Geophys Res, 90: 10487–10495
Peng L, Gao W, Geng F, Ran L, Zhou H. 2011, Analysis of ozone vertical distribution in Shanghai area (in Chinese with English abstract). Acta Sci Nat Univ Peking, 47: 805–811
Persson B R R, Holm E. 2014. ^{7}Be, ^{210}Pb, and ^{210}Po in the surface air from the Arctic to Antarctica. J Environ Radioact, 138: 364–374
Pham M K, Betti M, Nies H, Povinec P P. 2011. Temporal changes of ^{7}Be, ^{137}Cs and ^{210}Pb activity concentrations in surface air at Monaco and their correlation with meteorological parameters. J Environ Radioact, 102: 1045–1054
Pham M K, Povinec P P, Nies H, Betti M. 2013. Dry and wet deposition of ^{7}Be, ^{210}Pb and ^{137}Cs in Monaco air during 1998–2010: Seasonal variations of deposition fluxes. J Environ Radioact, 120: 45–57
Poet S E, Moore H E, Martell E A. 1972. Lead 210, bismuth 210, and polonium 210 in the atmosphere: Accurate ratio measurement and application to aerosol residence time determination. J Geophys Res, 77: 6515–6527
Rastogi N, Sarin M M. 2008. Atmospheric ^{210}Pb and ^{7}Be in ambient aerosols over low- and high-altitude sites in semiarid region: Temporal variability and transport processes. J Geophys Res, 113: D11103
Su C C, Huh C A, Lin F J. 2003. Factors controlling atmospheric fluxes of ^{7}Be and ^{210}Pb in northern Taiwan. Geophys Res Lett, 30: 2018
Tanoue M, Ichiyanagi K, Yoshimura K, Shimada J, Hirabayashi Y. 2017. Estimation of the isotopic composition and origins of winter precipitation over Japan using a regional isotope circulation model. J Geophys Res-Atmos, 122: 11621–11637
Tateda Y, Iwao K. 2008. High ^{210}Po atmospheric deposition flux in the subtropical coastal area of Japan. J Environ Radioact, 99: 98–108
Turekian K K, Graustein W C. 2003. Natural radionuclides in the atmosphere. In: Holland H D, Turekian K K, eds. Tretise on Geochemistry. New York: Elsevier. 261–279
Uğur A, Özden B, Filizok I. 2011. Determination of ^{210}Po and ^{210}Pb concentrations in atmospheric deposition in İzmir (Aegean sea-Turkey). Atmos Environ, 45: 4809–4813
Wang Z. 2014. Role of cumulus congestus in tropical cyclone formation in a high-resolution numerical model simulation. J Atmos Sci, 71: 1681–1700
Yamamoto M, Sakaguchi A, Sasaki K, Hirose K, Igarashi Y, Kim C K. 2006. Seasonal and spatial variation of atmospheric ^{210}Pb and ^{7}Be deposition: Features of the Japan Sea side of Japan. J Environ Radioact, 86: 110–131
Yamanaka T, Shimada J, Miyaoka K. 2002. Footprint analysis using event-based isotope data for identifying source area of precipitated water. J Geophys Res, 107: 4624
Yang F, Ye B, He K, Ma Y, Cadle S H, Chan T, Mulawa P A. 2005. Characterization of atmospheric mineral components of $PM_{2.5}$ in Beijing and Shanghai, China. Sci Total Environ, 343: 221–230

(Responsible editor: Jianfang HU)